EURASIP Journal on Advances in Signal Processing

RESEARCH Open Access

A wavelet selection scheme in underwater discharge signal analysis

Xiaobing Zhang[1], Binjie Lu[1,2*†] and Liang Qiao[3†]

†Binjie Lu and Liang Qiao contributed equally to this work.

*Correspondence: 757835764@qq.com

[1] College of Weapons Engineering, Naval University of Engineering, Jiefang Avenue, Wuhan 430033, Hubei, China
[2] The 92279 Unit of the PLA, Lai Street, Yantai 264003, Shandong, China
[3] School of Electrical and Electronic Engineering, Baoji University of Arts and Sciences, Baoguang Road, Baoji 721016, Shaanxi, China

Abstract

The analysis of underwater discharge signals is of great significance for its application. Wavelet-based de-noising and analysis technology is an effective means to study underwater discharge signals. The selection of wavelets is the key to the accuracy of wavelet analysis. A scheme of wavelet selection is provided in this paper. Based on the signal characteristics and actual noise, the reference target signal and noisy signal are constructed to ensure the accuracy of wavelet performance evaluation. Cross-correlation coefficient, root mean square error, signal-to-noise ratio, and smoothness are chosen as evaluation indexes and fused by the coefficient of variation method. The selected optimal wavelet is used to process the underwater wire-guided discharge signals. The results show that the scheme is feasible and practical.

Keywords: Signal processing, Wavelet, Underwater discharge, Time–frequency analysis, De-noising

1 Introduction

Underwater discharge explosions are widely utilized in industrial applications, such as underwater acoustic sources [1], water sterilization [2], marine exploration [3], and lithotripsy [4]. The time–frequency characteristics of shockwaves induced by the pulsed discharge in liquids are of the most concern. Accurate analysis of the signal characteristics is helpful in improving utilization efficiency.

The mechanism of underwater discharge is as follows [5]: When the underwater discharge starts, due to the enormous energy instantly released, the wire or the water between the discharge electrodes will quickly be heated, vaporize, plasma, and cause an explosion; the impact pressure can be up to 1000–10,000 atm. As the explosion's duration is short, this high pressure can compress the water medium around, creating a sudden change of pressure and density, thus creating a mighty shock wave and the outward propagation of supersonic speed. Then the plasma cools down and oscillates as a bubble several times. The bubble pulsations lag behind shock waves by milliseconds and overlap in the time domain.

The underwater discharge acoustic signal has a short time duration, high pressure, and wide frequency band. So the traditional Fourier transform method is not suitable. HHT (Hilbert–Huang Transform) method can be used to analyze such transient signals. Still,

modal aliasing may occur [6] so that the signal components' reconstruction and analysis at a specific frequency band are intractable. The wavelet analysis method is also suitable for studying this kind of signal and is convenient for local analysis [7, 8]. Wavelet transforms (WTs) use wavelets instead of sinusoids to convert a signal from the time to the time–frequency domain, revealing the time-support of frequencies, and intelligently exploring different frequency bands based on adaptive window lengths and positions [9]. The main types of wavelet transform are the Continuous Wavelet Transform (CWT), the Discrete Wavelet Transform (DWT), the Discrete-Time Wavelet Transform (DTWT), and the Stationary Discrete-Time Wavelet Transform (SDTWT). Each of them has a different way of working and is suitable for specific situations [10]. Chebyshev wavelet bases use orthogonal bases to transform the studied problems into linear or nonlinear Algebraic equation to simplify the calculation process and have been widely used to deal with various boundary conditions and solve integrodifferential equation equations. [11]. Guido et al. [12] introduced the Discrete Path Transform (DPT) to improve the regular Energy based workload analysis and the traditional zero-crossing rate-based spectral description. Yang et al. [13] proposed a novel and effective method called wavelet transform-based smooth ordering (WTSO) for HSI classification, which consists of three main components: wavelet transform for feature extraction, spectral–spatial based similarity measurement, smooth ordering-based 1D embedding, and construction of final classifier using interpolation scheme. Zheng et al. [14] established an adaptive multiscale graph wavelet decomposition (AMGWD) framework by taking the downsampling unbalance and also the high-pass componentsinto account. Guariglia et al. [15] provided the Weierstrass-Mandelbrot function(WMF) on the Cantor set, the wavelet spectrum and scalogram of the WMF could open new and interesting prospects. Guariglia and Silvestrov [16] described a wavelet expansion theory for positive definite distributions over the real line and defined a fractional derivative operator for complex functions in the distribution sense, which had already given some results in analytic number theory and could be able to describe different physical phenomena.

However, the main problem of this method is to choose the appropriate wavelet basis and the appropriate decomposition level when de-noising. Wavelet selection has a remarkable effect on de-noising performance and reconstruction accuracy. A specific wavelet filter has a specific frequency and phase response to the signal [17, 18]. The selection of the appropriate wavelet basis function is the premise of wavelet analysis. Using different wavelets to process the same signal will get different results, sometimes even very different. The required wavelet should be selected according to the specific situation to obtain accurate results. The improper wavelet will lead to serious deviation of signal analysis results from the real situation.

There have been some research results on this issue. Ma et al. [19] proposed a method for optimal wavelet selection based on prior knowledge of the partial discharge (PD) pulse shape: Correlation Based Wavelet Selection(CBWS). Suppose the correlation between the wavelet and the target signal is the largest among all the selectable wavelets and the target signal. In that case, the base wavelet is selected as the optimal signal de-noising. Li et al. [20] presented an automatic and scale-dependent base wavelet selection scheme for PD signal de-noising: Energy Based Wavelet Selection(EBWS). The energy criterion of the scale-dependent wavelet selection

scheme is proposed based on the energy percentage of PD signal and white noise decomposed at different scales. Liu et al. [21]proposed a Wavelet Entropy-Based Wavelet Selection Scheme (WEBWSS) to provide an alternative to CBWS and EBWS for partial discharge signal de-noising. Garg [22] introduced an automatic wavelet function selection algorithm: Mother Wavelet Selection (MWS) algorithm. The problem is formulated as an optimization criterion, and variance and genetic algorithm analysis are used to determine the optimal wavelets. Omari et al. [23] presented an automatic wavelet selection scheme, which was applied in PCG de-noising operation. The proposed method is based on multiplying the detail coefficients by the exponential approximation coefficients, or EXP for short, searching for the mother wavelet that provides the minimum value at each level and then selecting the wavelet and decomposition level regarding the highest EXP value. Peng et al. [24] analyzed the frequency characteristics of wavelets by mathematical modeling and selected the optimal wavelet base function hierarchically according to the amplitude-frequency characteristics of ECG signal. Du et al. [25] proposed the concept of information loss assessing coefficient on the foundation of some contents of wavelet threshold de-noising for the first time. To choose a suitable combination of scales, Wang et al. [26] proposed a rule to combine wavelet scales based on the sensitivity of each scale and selected the appropriate combination of wavelet scales based on sequence combination analysis (SCA). Instead of using correlation-based wavelet base selection for de-noising PD data, Altay et al. [27] introduced a wavelet selection method based on the most informative sub-band energy and entropy for separating noise from PD pulses. Wijaya et al. [28] proposed Information Quality Ratio (IQR) as a new metric for mother wavelet selection in real-world applications. IQR emphasizes that the reconstructed signal must maintain the essential information of the original signal. Wu et al. [29] presented a wavelet choice criterion to choose an appropriate mother wavelet that can make the energy-to-entropy of the wavelet coefficients maximum. The typical evaluation indexes to evaluate the performance of wavelets are the correlation coefficient, root mean square error, signal-to-noise ratio, and smoothness [30, 31]. There are also some effective index fusion methods in statistics [32].

Most of these previous research results are level by level and detailed analysis of a single specific signal, achieving very accurate results. Still, the efficiency is not high enough. A selection scheme that can select a wavelet with acceptable analysis accuracy and certain generality is necessary when a large number of signals need to be processed.

This study focuses on the selection of wavelets for the underwater discharge signal analysis. A scheme of wavelet selection based on typical discharge signal characteristics is given. According to the waveform characteristics of the signal to be analyzed, a waveform is generated by simulation as a reference target signal, and the actual noise is added to form a noisy signal. The reference signal and noise are known and consistent with the actual situation, ensuring the accuracy and credibility of performance evaluation. The optional wavelets are used to denoise the noisy signal, and the performance of each wavelet is evaluated according to the evaluation indexes to select the most suitable wavelet for analyzing this kind of signal. Then underwater discharge signals produced by the electric explosion of different wires were processed by the chosen optimal wavelet. The results show that the scheme is feasible and practical.

2 Method and experimental setup

2.1 Optional wavelets and decomposition levels

The wavelets have attributes such as orthogonality, biorthogonality, compact support, and vanishing moment [7]. Orthogonality and biorthogonality are conducive to accurate signal reconstruction. Compact support can ensure excellent local time–frequency characteristics. Wavelet basis with certain vanishing moment order can effectively highlight the singularity of signal, which is very beneficial to signal de-noising. The attributes of common wavelets are shown in Table 1.

As mentioned earlier, the underwater discharge signal has the characteristics of short time duration, high pressure, and wide frequency band, which requires that the wavelets used to process such signals have the properties of orthogonality or biorthogonality, compact support, symmetry, and particular vanishing moment. The Discrete-Time Wavelet Transform (DTWT) is used to process the signal. Then the Daubechies, Symlets, Coiflets, Biorthogonal, and Revers Biorthogonal wavelet families are selected as optional wavelets to process the underwater discharge signal. Waveforms of some wavelets are shown in Fig. 1.

There is a maximum decomposition level for a certain length of data and a specific wavelet. So the optional decomposition levels should not be more than the maximum level. The larger the decomposition level, the more obvious the different characteristics of noise and signal, which is more conducive to their separation. On the other hand, the larger the decomposition level, the greater the distortion of the reconstructed signal, which will affect the final de-noising effect to a certain extent.

2.2 The evaluation indexes of wavelet selection

The key to indexes selection is identifying quantitative expressions that can characterize the de-noised signal from different perspectives. Existing metrics for characterizing

Table 1 The attributes of common wavelets

	Orthogonal	Biorthogonal	Compact support	Symmetry	Vanishing moment	CWT	DWT
Morlet	No	No	No	Yes	–	Yes	No
Meyer	Yes	Yes	No	Yes	–	Yes	Yes
Haar	Yes	Yes	Yes	Yes	1	Yes	Yes
Daubechies	Yes	Yes	Yes	Approx	N	Yes	Yes
Symlets	Yes	Yes	Yes	Approx	N	Yes	Yes
Coiflets	No	Yes	Yes	Approx	2N	Yes	Yes
Biorthogonal	No	Yes	Yes	Yes	Nr	Yes	Yes
Revers Biorthogonal	No	Yes	Yes	Yes	Nd	Yes	Yes

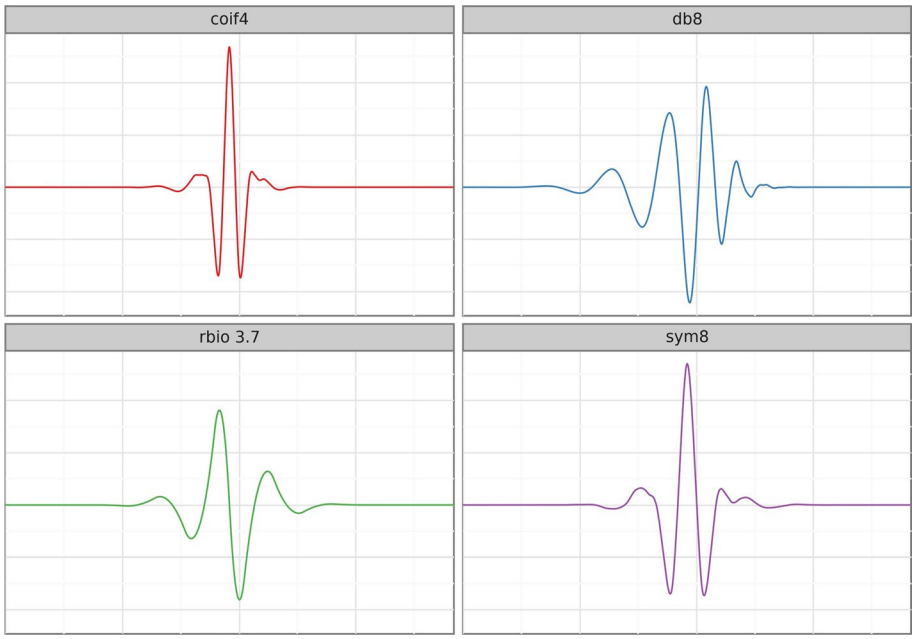

Fig. 1 Waveforms of some wavelets

wavelet de-noised signals include root mean square error, signal to noise ratio, number of correlations, and smoothness [30, 31].

2.2.1 Cross-correlation coefficient (CC)

$$\mathrm{CC} = \frac{\sum_{n=1}^{N}(s(n)-\bar{s}(n))(s_r(n)-\bar{s}_r(n))}{\sqrt{\sum_{n=1}^{N}(s(n)-\bar{s}(n))^2 \sum_{n=1}^{N}(s_r(n)-\bar{s}_r(n))^2}} \tag{1}$$

where N is the data length, $s(n)$ and $s(n)_r$ are the pure signal and the wavelet-processed and re-constructed signal; $\bar{s}(n)$ and $\bar{s}_r(n)$ are the mean values of $s(n)$ and $s_r(n)$.

2.2.2 Root mean square error (RMSE)

$$\mathrm{RMSE} = \sqrt{\frac{1}{N}\sum_{n=1}^{N}[s(n)-s_r(n)]^2} \tag{2}$$

This index reflects the degree of difference between s and s_r. Smaller RMSE values indicate better results.

2.2.3 Signal-to-noise ratio (SNR)

$$\begin{aligned} \text{power}_{\text{signal}} &= \frac{1}{N}\sum_{n=1}^{N}[s(n)]^2 \\ \text{power}_{\text{noise}} &= \frac{1}{N}\sum_{n=1}^{N}[\text{noise}(n)]^2 \\ \text{SNR} &= 10\text{lg}\left(\frac{\text{power}_{\text{signal}}}{\text{power}_{\text{noise}}}\right) \end{aligned} \tag{3}$$

where noise(n) is the noise. $\text{power}_{\text{signal}}$ and $\text{power}_{\text{noise}}$ are the power of pure signal and noise. It is generally accepted that a higher *SNR* means a better result.

2.2.4 Smoothness(r)

$$r = \frac{\sum_{n=1}^{N-1}[s_r(n+1) - s_r(n)]^2}{\sum_{n=1}^{N-1}[s(n+1) - s(n)]^2} \tag{4}$$

Smaller smoothness values indicate better de-noising results.

Accordingly, it can be inferred that [32]: the CC reflects the fitting information of the reconstructed signal to the pure signal; the RMSE actually reflects the overall deviation information of the signal; the SNR ratio reflects the effect of the noise information on the overall signal; and the r reflects the local variation information of the signal, i.e., whether there are more local mutations. These four indexes are independent of each other. The pursuit of the high performance of a single index will often lead to the decline of the performance of other indicators. For example, only the pursuit of high SNR will often lead to the deterioration of CC and RMSE.

3 The method of index fusion

One typical problem is the fusion of various evaluation indexes. Some previous studies have chosen only one measure, usually RMSE, so there is no index fusion problem. But there is no doubt that multi-index evaluation can obtain a better result. The usual method is to assign a certain weight to each indicator and then perform a weighted fusion. Some literature uses manual subjective assignment of weights, but the reasonableness of the weights determined by this method remains controversial. There are now several methods for objectively determining weights in statistics. Shen et al. [30] used the coefficient of variation method to assign weights and fuse indicators automatically. Tao et al. [32] used the entropy value method to weight the indicators for fusion. Both of the two methods assume that if the variation degree of an index value is greater, the dispersion degree of the index will be more significant, the influence of the index on the comprehensive evaluation will be more powerful, and the weight of the index should be greater; vice versa. This study used the coefficient of variation method [33] to fuse the indexes. Analysis using the entropy method was also carried out later, and the results were the same as the coefficient of variation method, so they are not listed in the text. The main steps of the coefficient of variation method are:

- *Step1* Use the min−max algorithm to normalize the data sets of the four evaluation parameters, as follows:

$$\mathrm{CC}_m(i) = \frac{\mathrm{CC}(i) - \min(\mathrm{CC})}{\max(\mathrm{CC}) - \min(\mathrm{CC})} \tag{5}$$

$$\mathrm{RMSE}_m(i) = \frac{\mathrm{RMSE}(i) - \min(\mathrm{RMSE})}{\max(\mathrm{RMSE}) - \min(\mathrm{RMSE})} \tag{6}$$

$$\mathrm{SNR}_m(i) = \frac{\mathrm{SNR}(i) - \min(\mathrm{SNR})}{\max(\mathrm{SNR}) - \min(\mathrm{SNR})} \tag{7}$$

$$r_m(i) = \frac{r(i) - \min(r)}{\max(r) - \min(r)} \quad (i = 1, 2, \ldots, M) \tag{8}$$

where M is the length of the index dataset. $\mathrm{CC}(i)$, $\mathrm{RMSE}(i)$, $\mathrm{SNR}(i)$ and $r(i)$ are the cross-correlation coefficient, root mean square error, signal-to-noise ratio and smoothness before normalize. $\mathrm{CC}_m(i)$, $\mathrm{RMSE}_m(i)$, $\mathrm{SNR}_m(i)$ and $r_m(i)$ are the CC, RMSE, SNR and r after normalize. min() is the minimum value of the evaluation index data set before normalization, max() is the maximum value of the evaluation index data set before normalization.

- *Step2* Calculate the coefficient of variation of each normalized evaluation index data set:

$$\mathrm{CV}_{\mathrm{EI}_k} = \frac{\sigma_{\mathrm{EI}_k}}{\mu_{\mathrm{EI}_k}} \qquad (k = 1, 2, 3, 4) \tag{9}$$

where $\mathrm{CV}_{\mathrm{EI}_k}$ is the coefficient of variation of each normalized evaluation index data set, σ_{EI_k} and μ_{EI_k} are the standard deviation and mean value of each normalized evaluation index data set. EI_1, EI_2, EI_3, EI_4 represent CC_m, RMSE_m, SNR_m and r_m, respectively.

- *Step3*:Obtain the weight of each normalized evaluation parameter data set.

$$W_{\mathrm{EI}_k} = \frac{\mathrm{CV}_{\mathrm{EI}_k}}{\sum_{k=1}^{4} \mathrm{CV}_{\mathrm{EI}_k}} \tag{10}$$

where W_{EI_k} is the weight of each evaluation index data set.

- *Step4* Calculate the comprehensive evaluation index (CEI) with different combinations of optional wavelets and decomposition levels by weight:

$$\mathrm{CEI}(i) = \sum_{k=1}^{4} W_{\mathrm{EI}_k} \times \mathrm{EI}_k(i) \tag{11}$$

where $\mathrm{CEI}(i)$ is the comprehensive evaluation index of the ith combination of optional wavelets and decomposition levels. The combination with the highest CEI shows the best result.

3.1 The scheme of wavelet selection

To select the optimal wavelet accurately, the evaluation index must be accurate and effective. Evaluation indexes are mainly calculated from the pure signal, noise, and processed noisy signal. The accurate acquisition of pure signal and noise is the key to ensure the indexes' accuracy and credibility. But in practical application, the pure signal is usually undetectable. It is obviously inappropriate to use the measured signal as the noisy signal and the wavelet processed signal as the reference signal.

Fortunately, typical waveform characteristics of many signals are known based on the mechanisms of signal generation. The typical reference waveform of underwater discharge signal is shown in Fig. 2. It consists of shock wave and subsequent bubble pulsations.

Whether in the anechoic pool or in the outdoor lake or ocean, the noise of underwater discharge signals can be measured. The noise characteristics may be different in different environments, but they are basically stable in the short time of the underwater discharge. Blanks at the beginning or the end of the signal can be considered pure noise signals (shown in Fig. 3) and superimposed with the reference waveform to generate a simulated noise signal. The pure signal and noise in the simulated signal can be considered known. The instrument measurement error is considered as stable during the very short duration time of underwater discharge. By processing this signal, we can accurately calculate the evaluation index after the processing of each combination of wavelets and decomposition levels. The *CEI* can be calculated by fusing the indexes through the coefficient of variation method. Then the optimal wavelet can be selected. The scheme is shown in Fig. 4.

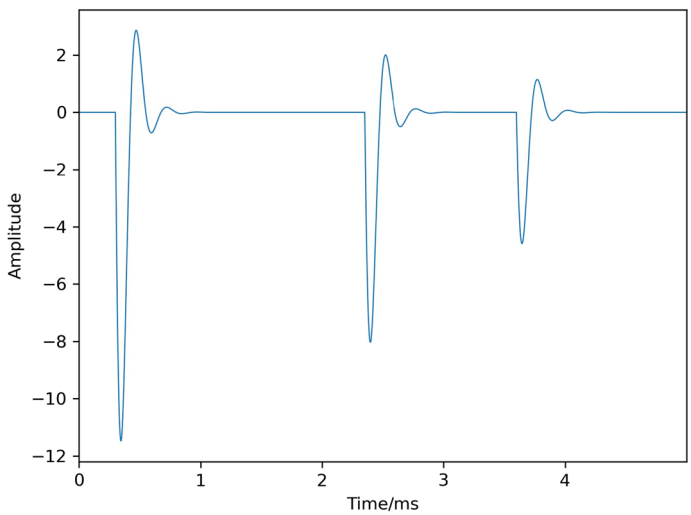

Fig. 2 Ideal reference waveform of underwater discharge

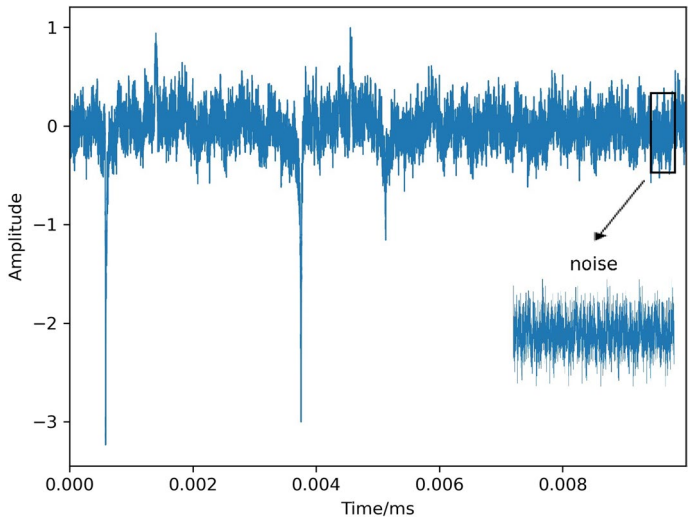

Fig. 3 Measured underwater discharge signal and noise

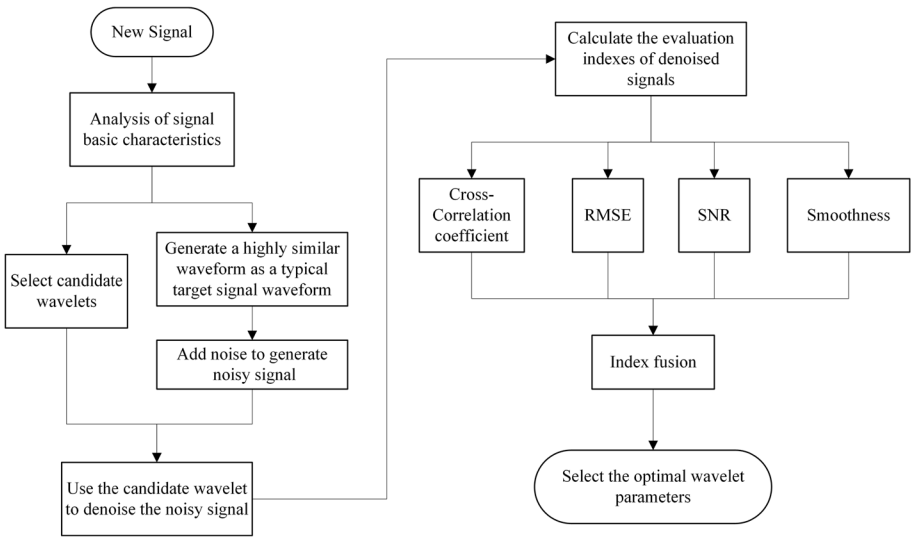

Fig. 4 Scheme of wavelet selection

3.2 Experiment setup

An experiment is implemented to compare the underwater wire-guided discharge discharge signals with different materials. A pair of 304 stainless steel cylindrical electrodes with 5 mm cross-section diameter and 150 mm length were fixed on a self-made plastic base to discharge. Gold, silver, and copper wires with a diameter of 0.05 mm and a length of 6 mm were fixed between the two electrodes and then placed at a depth of 1 m under the water of the anechoic pool. A high voltage pulse power drove the underwater plasma discharge system with a fixed output voltage of 10kV and an energy storage capacitor of 0.11mf. The explosive acoustic signals were collected by a hydrophone produced by the Hangzhou Institute of Applied Acoustics with a sensitivity of -205dB re 1V/mPa in the range of 5Hz-15MHz. A RIGOL MSO5354 digital storage oscilloscope recorded the

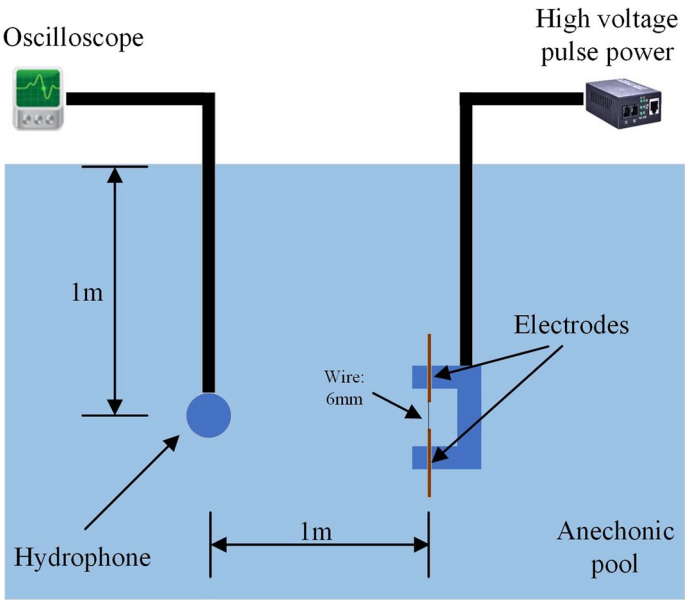

Fig. 5 Setup of the underwater wire-guided discharge experiment

collected sound signals. The water conductivity was 0.37mS/cm, and the water temperature was 17.5°C. The experiment setup is shown in Fig. 5.

4 Results

4.1 The selection of optimal wavelet

After computation, the *EI*s and *CEI* of each combination of wavelets and decomposition levels are obtained; some of them are shown in Table 2. From the *CEI*, the optimal wavelet is rbio3.7, and the optimal decomposition level for de-noising is 9. The worst performing wavelet is ribo 3.1, which is mainly poor in signal-to-noise ratio and smoothness. The de-noising results are shown in Fig. 6.

Table 2 *EI*s and *CEI*s of some combination of wavelets and decomposition levels

Wavelet	Decomposition level	CC	RMSE	SNR	*r*	CEI
rbio 3.7	9	0.9983	0.0952	24.7679	0.0213	0.9984
bior 5.5	9	0.9982	0.0971	24.5919	0.0196	0.9803
sym4	9	0.9978	0.1065	23.7894	0.0254	0.8909
db8	9	0.9979	0.1058	23.8483	0.0323	0.8959
coif4	8	0.9979	0.1039	24.0022	0.0251	0.9148
rbio 3.1	7	0.9935	0.1849	18.9998	0.8658	0.0054

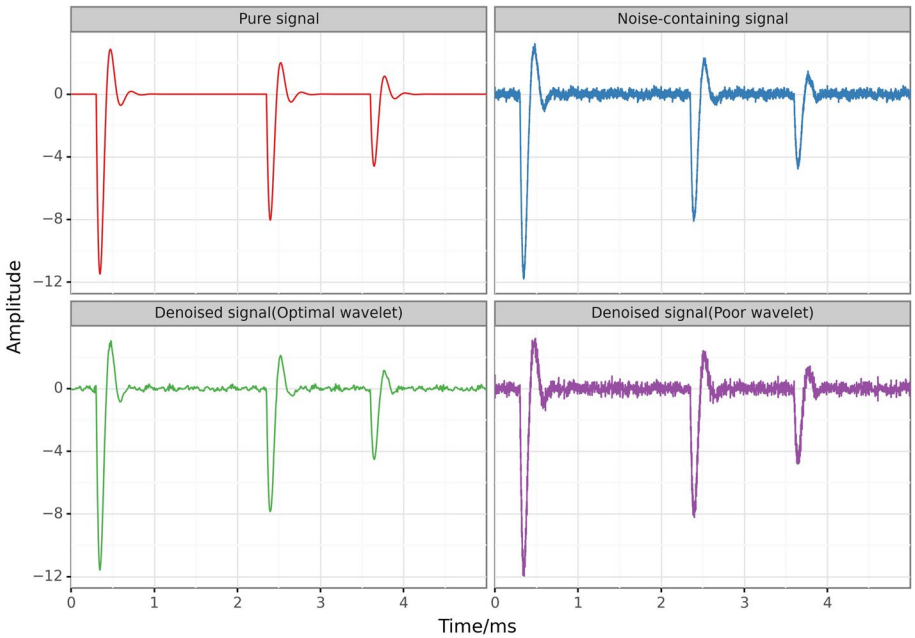

Fig. 6 The effect of denoising using optimal and poor wavelets

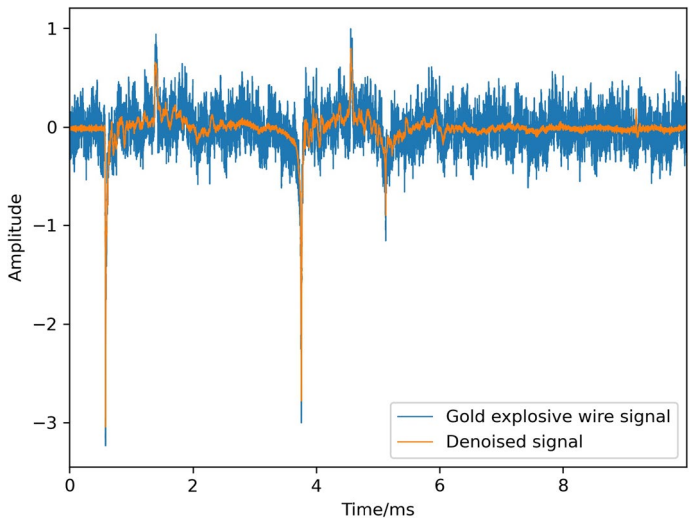

Fig. 7 The underwater gold wire discharge signal and the de-noised signal

4.2 Wavelet-based processing of underwater wire-guided discharge discharge signals

Using the selected optimal wavelet, the measured underwater discharge signal is de-noised, and then wavelet packet decomposition is used to analyze the energy distribution in each frequency band. It can be seen in Fig. 7 that the noise can be eliminated effectively after processing. Then the de-noised signals were decomposed by rbio 3.7 wavelet-packet at level 4. The reconstructed waveforms of wavelet packet

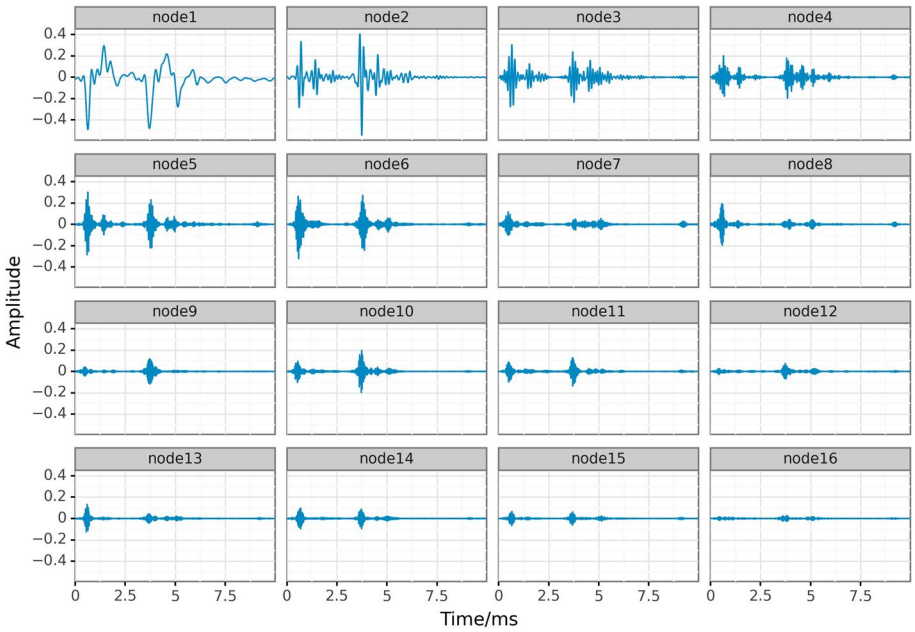

Fig. 8 Reconstructing wavelet packe node waveforms of discharge signal

Table 3 The frequency band of each wavelet packet node

Node	Frequency(Hz)	Node	Frequency(Hz)
1	0–3125	9	25,000–28,125
2	3125–6250	10	28,125–31,250
3	6250–9375	11	31,250–34,375
4	9375–12,500	12	34,375–37,500
5	12,500–15625	13	37,500–40,625
6	15,625–18,750	14	40,625–43,750
7	18,750–21,875	15	43,750–46,875
8	21,875–25,000	16	46,875–50,000

nodes are shown in Fig. 8. The sample rate is 10^5Hz, so the frequency band of each node is shown in Table 3.

It can be concluded from Fig. 8 that the waveforms of the first six nodes have greater amplitude. So the underwater wire-guided discharge signal has more low-frequency components.

4.3 The comparison of underwater wire-guided discharge discharge signals with different materials

The energy–frequency distributions of underwater wire-guided discharge discharge signals are obtained by using rbio 3.7 wavelet packet decomposition at level 5 and calculating the energy proportion of each node in the 5th layer. We can conclude from Fig. 9 that the gold wire explosive signal has more high-frequency components than copper and silver.

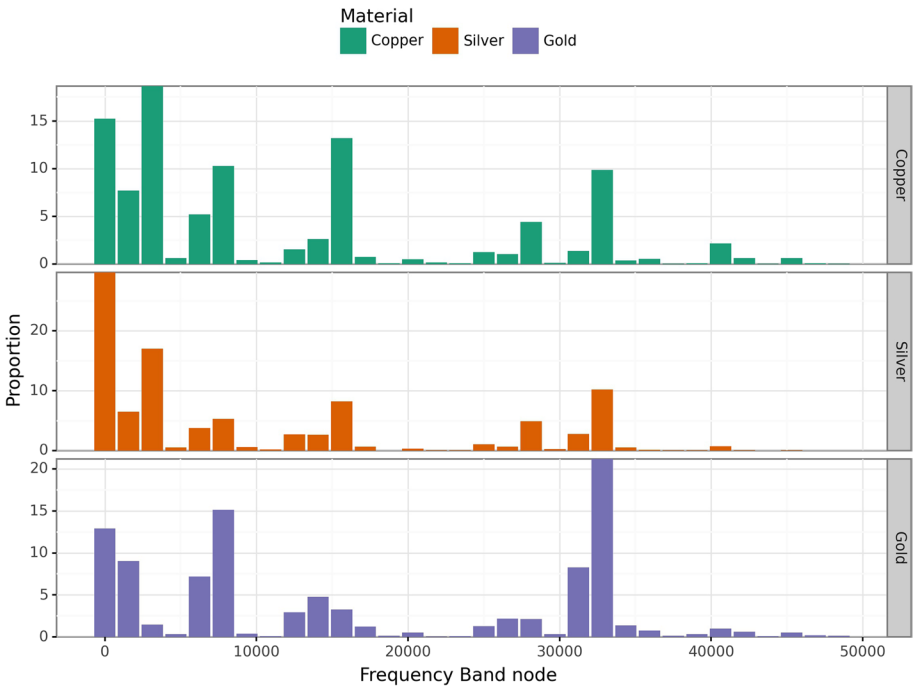

Fig. 9 Frequency–energy distributions of signals with different materials

5 Conclusions

In this study, a scheme of wavelet selection is provided. And the processing of underwater explosive signals using selected wavelets proved the effectiveness of the wavelet selection scheme. Based on prior knowledge, the reference waveform of the target signal can be fitted, and real noise is added to the fitted target signal to form a fitted noisy signal. Then the fitted noisy signal is processed by optional wavelets. The evaluation indexes after the processing of each combination of wavelets and decomposition levels are calculated, and the comprehensive evaluation indexes are obtained through the coefficient of variation method. Then the optimal wavelet can be selected. The underwater wire-guided explosive signals were de-noised by the optimal wavelet and decomposition level. Then wavelet packet decomposition of optimal wavelet was used to analyze the energy–frequency characteristics. The results proved the effectiveness of the wavelet selection scheme. The scheme is a general solution that can be applied to signals that have prior knowledge of approximate waveform characteristics, and the results of the selection can be used for a class of signals with similar signal characteristics. The selection of threshold in de-noising involves noise characteristics, which is not within the scope of this paper.

Acknowledgements

The experimental environment and measuring instruments are provided by Chongqing Qianwei Technology Group Co., Ltd.

Author contributions

XZ and LQ conceived the experiments, BL and LQ conducted the experiments and analysed the results, LQ prepared the necessary equipment and materials. LQ prepared the main body of the manuscript, XZ revised the manuscript. All authors reviewed the manuscript.

Funding
This research is funded by the "14th Five Year Plan" pre research project.

Availability of data and materials
The datasets used and/or analysed during the current study are available from the corresponding author on reasonable request.

Declarations

Competing interests
The authors declare that they have no competing interests.

Received: 30 March 2023 Accepted: 9 October 2023
Published online: 24 October 2023

References

1. L.H. Fry, P. Adair, R. Williams, Long life sparker for pulse powered underwater acoustic transducer. In: Digest of Technical Papers. 12th IEEE International Pulsed Power Conference. (Cat. No.99CH36358), vol. 2 (IEEE, Monterey, 1999) p. 781–784. https://doi.org/10.1109/PPC.1999.823630 . http://ieeexplore.ieee.org/document/823630/ Accessed 2021-01-31
2. K. Shang, J. Li, R. Morent, Hybrid electric discharge plasma technologies for water decontamination: a short review. Plasma Sci. Technol. **21**(04), 5–13 (2019). https://doi.org/10.1088/2058-6272/aafbc6
3. Y. Huang, L. Zhang, Y. Hui, X. Zhu, K. Yan, Experimental study of the electric pulse-width effect on the acoustic pulse of a plasma sparker. IEEE J. Ocean. Eng. **99**, 1–7 (2016). https://doi.org/10.1109/JOE.2015.2471635
4. Z. Xu, L. Wang, N. Zhang, S. Deng, Y. Xu, X. Zhou, Clinical applications of plasma shock wave lithotripsy in treating post-operative remnant stones impacted in the extra- and intrahepatic bile ducts. Surg. Endosc. **16**(4), 646 (2002). https://doi.org/10.1007/s00464-001-8146-2//
5. Y. Wang, Theoretical and experimental study of the underwater plasma acoustic source. PhD thesis, Graduate School of National University of Defense Technology. (2012)
6. N. Huang, S.S.P. Shen, *Hilbert–Huang Transform and Its Applications* (World Scientific, 2005). https://doi.org/10.1142/5862
7. I. Daubechies, C. Chui, Functional analysis. (book reviews: Ten lectures on wavelets; an introduction to wavelets). Science **257**, 821–822 (1992). https://doi.org/10.1126/science.257.5071.821
8. E. Guariglia, R.C. Guido, G.J.P. Dalalana, From wavelet analysis to fractional calculus: a review. Mathematics (2023). https://doi.org/10.3390/math11071606
9. R.C. Guido, Wavelets behind the scenes: practical aspects, insights, and perspectives. Phys. Rep. **985**, 1–23 (2022). https://doi.org/10.1016/j.physrep.2022.08.001
10. R.C. Guido, F. Pedroso, A. Furlan, R.C. Contreras, L.G. Caobianco, J.S. Neto, Cwt × dwt × dtwt × sdtwt: clarifying terminologies and roles of different types of wavelet transforms. Int. J. Wavel. Multiresolut. Inf. Process. **18**(06), 2030001 (2020). https://doi.org/10.1142/S0219691320300017
11. E. Guariglia, R.C. Guido, Chebyshev wavelet analysis. J. Funct. Spaces **2022**, 5542054 (2022). https://doi.org/10.1155/2022/5542054
12. R.C. Guido, F. Pedroso, R.C. Contreras, L.C. Rodrigues, E. Guariglia, J.S. Neto, Introducing the discrete path transform (DPT) and its applications in signal analysis, artefact removal, and spoken word recognition. Digit. Sign. Process. **117**, 103158 (2021). https://doi.org/10.1016/j.dsp.2021.103158
13. L. Yang, H. Su, C. Zhong, Z. Meng, H. Luo, X. Li, Y.Y. Tang, Y. Lu, Hyperspectral image classification using wavelet transform-based smooth ordering. Multiresolut. Inf. Process. **17**(06), 1950050 (2019). https://doi.org/10.1142/S0219691319500504
14. X. Zheng, Y.Y. Tang, J. Zhou, A framework of adaptive multiscale wavelet decomposition for signals on undirected graphs. IEEE Trans. Sign. Process. **67**(7), 1696–1711 (2019). https://doi.org/10.1109/TSP.2019.2896246
15. E. Guariglia, Spectral analysis of the weierstrass–mandelbrot function. In: 2017 2nd International Multidisciplinary Conference on Computer and Energy Science (SpliTech), pp 1–6 (2017)
16. E. Guariglia, S. Silvestrov, Fractional-wavelet analysis of positive definite distributions and wavelets on D′(C) D′(C), in *Engineering Mathematics II*. ed. by S. Silvestrov, M. Rančić (Springer, Cham, 2016), pp.337–353
17. R.C. Guido, Practical and useful tips on discrete wavelet transforms [sp tips & tricks]. IEEE Sign. Process. Mag. **32**(3), 162–166 (2015). https://doi.org/10.1109/MSP.2014.2368586
18. R.C. Guido, Effectively interpreting discrete wavelet transformed signals [lecture notes]. IEEE Sign. Process. Mag. **34**(3), 89–100 (2017). https://doi.org/10.1109/MSP.2017.2672759
19. X. Ma, C. Zhou, I.J. Kemp, Automated wavelet selection and thresholding for pd detection. Electr. Insul. Mag. IEEE **18**(2), 37–45 (2002). https://doi.org/10.1109/57.995398
20. J. Li, T. Jiang, S. Grzybowski, C. Cheng, Scale dependent wavelet selection for de-noising of partial discharge detection. IEEE Trans. Dielectr. Electr. Insula. **17**, 1705–1714 (2011). https://doi.org/10.1109/TDEI.2010.5658220
21. J. Liu, W.H. Siew, J. Soraghan, E. Morris, A novel wavelet selection scheme for partial discharge signal detection under low snr condition. In: 2018 IEEE Conference on Electrical Insulation and Dielectric Phenomena (CEIDP), pp. 498–501 (2018). https://doi.org/10.1109/CEIDP.2018.8544802
22. G. Garg, A signal invariant wavelet function selection algorithm. Med. Biol. Engi. Comput. (2015). https://doi.org/10.1007/s11517-015-1354-z
23. O. Tahar, F. Reguig, An automatic wavelet denoising scheme for heart sounds. Int. J. Wavel. Multiresolut. Inf. Process. **13**, 150406005741006 (2015). https://doi.org/10.1142/S0219691315500162
24. Z. Peng, G. Wang, Study on optimal selection of wavelet vanishing moments for ECG denoising. Sci. Rep. (2017). https://doi.org/10.1038/s41598-017-04837-9

25. D. ZhaoHeng, L. ShangHe, W. Lei, Selection of the optimal wavelet bases for wavelet de-noising of partial discharge signal. In: 2010 2nd International Conference on Signal Processing Systems, vol. 3, pp. 3–4003404 (2010). https://doi.org/10.1109/ICSPS.2010.5555675
26. K. Wang, X. Zhang, J. Ota, Y. Huang, Estimation of handgrip force from semg based on wavelet scale selection. Sensors **18**, 663 (2018). https://doi.org/10.3390/s18020663
27. O. Altay, Z. Kalenderli, Wavelet base selection for de-noising and extraction of partial discharge pulses in noisy environment. IET Sci. Measurement Technol. (2014). https://doi.org/10.1049/iet-smt.2013.0114
28. D. Wijaya, R. Sarno, E. Zulaika, Information quality ratio as a novel metric for mother wavelet selection. Chemom. Intell. Lab. Syst. (2016). https://doi.org/10.1016/j.chemolab.2016.11.012
29. C. Wu, T. Chen, R. Jiang, L. Ning, Z. Jiang, A novel approach to wavelet selection and tree kernel construction for diagnosis of rolling element bearing fault. J. Intell. Manuf. (2015). https://doi.org/10.1007/s10845-015-1070-4
30. Y. Shen, J. Gao, L. Sun, S. Zhao, CN110599425A: A Wavelet Parameter Selection Method for ACFM Signal Wavelet Denoising
31. Z. Li, Y. Deng, G. Zhang, X. Yang, Determination of best grading of wavelet transform in deformation measurement data filtering. Geomat. Inf. Sci. Wuhan Univ. **36**, 285–288 (2011)
32. K. Tao, J. Zhu, A hybrid indicator for determining the best decomposition scale of wavelet denoising. Cehui Xuebao/Acta Geodaetica et Cartographica Sinica **41**, 749–755 (2012)
33. R.E. McAuliffe, *Coefficient of Variation* (American Cancer Society, 2015). https://doi.org/10.1002/9781118785317.weom080117

Publisher's Note